Structure
Article

A β Strand Lock Exchange for Signal Transduction in TonB-Dependent Transducers on the Basis of a Common Structural Motif

Karl Brillet,[1] Laure Journet,[1] Hervé Célia,[1] Laetitia Paulus,[1] Aude Stahl,[1] Franc Pattus,[1] and David Cobessi[1,*]
[1]Institut Gilbert-Laustriat, UMR7175 CNRS/Université Louis Pasteur, Strasbourg I, Département Récepteurs et Protéines Membranaires, Ecole Supérieure de Biotechnologie de Strasbourg, Boulevard Sébastien Brandt, BP 10413, F-67412 Illkirch, France
*Correspondence: cobessi@esbs.u-strasbg.fr
DOI 10.1016/j.str.2007.08.013

SUMMARY

Transport of molecules larger than 600 Da across the outer membrane involves TonB-dependent receptors and TonB-ExbB-ExbD of the inner membrane. The transport is energy consuming, and involves direct interactions between a short N-terminal sequence of receptor, called the TonB box, and TonB. We solved the structure of the ferric pyoverdine (Pvd-Fe) outer membrane receptor FpvA from *Pseudomonas aeruginosa* in its apo form. Structure analyses show that residues of the TonB box are in a β strand which interacts through a mixed four-stranded β sheet with the periplasmic signaling domain involved in interactions with an inner membrane sigma regulator. In this conformation, the TonB box cannot form a four-stranded β sheet with TonB. The FhuA-TonB or BtuB-TonB structures show that the TonB-FpvA interactions require a conformational change which involves a β strand lock-exchange mechanism. This mechanism is compatible with movements of the periplasmic domain deduced from crystallographic analyses of FpvA, FpvA-Pvd, and FpvA-Pvd-Fe.

INTRODUCTION

Iron is an essential element for most living organisms (Posey and Gherardini, 2000) and necessary for the virulence of pathogenic Gram-negative bacteria. Although iron is one of the most abundant elements on earth, its bioavailability is very poor (Neilands, 1995): under aerobic conditions or at physiological pH, it precipitates to form insoluble iron oxy-hydroxide complexes. Its free concentration in biological fluids is very low (10^{-18} M), and less than that required for bacterial growth ($\sim 10^{-7}$ M to 10^{-8} M) (Stintzi et al., 2000). Under iron-limiting conditions, most bacteria synthesize and secrete iron chelators, called siderophores, which bind iron (III) and make it available for the cell (Ferguson and Deisenhofer, 2002). During infection, these iron siderophores, which are small molecules (MW 350–1500 Da), compete with iron storage proteins for iron. Iron siderophores, and other molecules larger than 600 Da such as vitamin B12, do not diffuse through the outer membrane passively and do not use nonspecific or substrate-specific porins for entry. Metal siderophores are transported by TonB-dependent receptors (Ferguson and Deisenhofer, 2002, 2004) using an energy-consuming mechanism involving interactions between the TonB box of the receptor and TonB of the TonB-ExbB-ExbD complex located in the inner membrane. In the crystal structure of two siderophore receptors (FhuA and BtuB) interacting with the C-terminal domain of TonB (Pro153–Asn233 in BtuB-TonB or Arg158–Thr235 in FhuA-TonB), the TonB box is folded into a β strand and interacts with the mixed three-stranded β sheet of the TonB periplasmic part, thereby forming a mixed four-stranded β sheet (Pawelek et al., 2006; Shultis et al., 2006).

Pseudomonas aeruginosa is an opportunistic human pathogen which infects injured, immunodeficient, or otherwise compromised patients. Under iron-limiting conditions, the bacterium secretes a major siderophore, pyoverdine (Pvd) (Poole and McKay, 2003). Pvd contributes to infection by competing with transferrin for iron, and thereby overcomes the iron-withholding mechanism present in mammals. The pyoverdine receptor, FpvA, is embedded in the outer membrane in a complex with Pvd (Schalk et al., 1999). FpvA belongs to the TonB-transducer family. Members of this family are TonB-dependent transporters with a signaling domain, upstream from the TonB box, which interacts with a sigma regulator of the inner membrane (Koebnik, 2005), called FpvR in *P. aeruginosa*. These transducers are able to regulate their own synthesis as well as that of their cognate siderophore, and this regulation depends solely on ferric siderophore binding (Braun et al., 2003; Schalk et al., 2004). The three-dimensional structures of the outer membrane transducer FecA from *Escherichia coli* (Ferguson et al., 2002; Yue et al., 2003) and FpvA from *P. aeruginosa* (Cobessi et al., 2005a) have now been solved. Structural studies of FpvA-Pvd-Fe are the only source so far of structural data on interactions of the signaling domain folded with the rest of the receptor (Wirth et al., 2007). In this structure,

Table 1. X-Ray Data Statistics

Wavelength (Å)	0.97565
Resolution (Å)	47.14–2.77 (2.92–2.77)
Space group	C2
Cell parameters (Å)	189.88, 128.78, 139.15, $\beta = 130.55^\circ$
Total reflections	248,120 (20,956)
Unique reflections	63,018 (7,865)
Completeness (%)	97.5 (83.7)
I/σI	13.7 (2.7)
R_{sym} (%)[a]	8.0 (39.1)

Values in parentheses correspond to the statistics in the highest-resolution shell.
[a] $R_{sym} = \sum\sum|I_i - I_m|/\sum\sum I_i$, where I_i is the intensity of the measured reflection and I_m is the mean intensity of this reflection.

Table 2. Refinement and Model Statistics

Resolution range (Å)	30.47–2.77 (2.84–2.77)
Number of reflections used for R_{cryst} calculation	56,582 (3,041)
Number of reflections used for R_{free} calculation	3,195 (184)
Data cutoff F/σ_F	0.0
R_{cryst} value (%)[a]	20.77 (29.9)
R_{free} value (%)	24.72 (33.0)
Number of nonhydrogen protein atoms	12,110
Number of phosphate ions	10
Mean B factors, protein main-chain atoms (Å^2)	39.87
Mean B factors, protein side-chain atoms (Å^2)	40.88
Ramachandran plot	
Residues in most favored regions (%)	87.7
Residues in additionally allowed regions (%)	11.4
Residues in generously allowed regions (%)	0.8
Residues in disallowed regions (%)	0.0
Rms differences from ideal geometry	
Bond length (Å)	0.011
Bond angle (°)	1.388

Values in parentheses correspond to the statistics in the highest-resolution shell.
[a] $R_{cryst} = \sum||F_{obs}| - |F_{calc}||/\sum|F_{obs}|$. R_{free} (Brunger, 1992) is the same as R_{cryst} but calculated for n% data omitted from the refinement where n is 5.1% for FpvA.

the TonB box was not observed in the electron density, and the loop of 20 residues connecting the signaling domain to the membrane part of the protein was also not found. The fold of the FpvA signaling domain is similar to those of FecA (Garcia-Herrero and Vogel, 2005; Wirth et al., 2007) and PupA from *Pseudomonas putida* (Ferguson et al., 2007) solved by NMR.

We report here the full-length crystal structure of a transducer where residues of the TonB box are in a β strand which forms a mixed four-stranded β sheet with the three-stranded β sheet of the signaling domain. In this conformation, the residues of TonB are buried between the signaling domain and the plug and barrel and cannot interact with TonB through a four-stranded β sheet. Interactions between TonB and the TonB box require structural changes of the receptor involving displacement of the signaling domain in the periplasm. This mechanism is strongly supported by structural comparisons and modeling based on the FhuA-TonB and BtuB-TonB structures.

RESULTS

Structural Differences in the Asymmetric Unit Reveal Structural Plasticity of FpvA

FpvA was crystallized in a solution containing between 1.3 and 1.4 M Na_2HPO_4 and 0.1 M MES (pH 6.5) in space group C2 (Table 1). Two molecules are in the asymmetric unit. The membrane part is involved in the intermolecular contacts in the asymmetric unit and the crystals are type II membrane protein crystals. The overall folding of the protein is consistent with the classical fold of TonB-dependent transducers: a 22 β-stranded barrel of which the lumen is occluded by the plug domain connected to the periplasmic signaling domain which displays a β-α-β fold (Wirth et al., 2007). The pH of the crystallization solution is 5.6 and several mono-anionic phosphate ions (Table 2) bound to glutamate carboxylate groups were identified in the $F_o - F_c$ electron density map.

Continuous electron density was observed from Gln44 to Phe815 in one molecule of the asymmetric unit (molecule A), whereas in the second (molecule B), the electron density covered from Gln44 to Val117 and from Gln136 to Phe815. The molecules can only be superimposed from Gln136 to Phe815. The root-mean-square deviation (rmsd) is 0.578 Å for the overall structure. The main difference between the two molecules is the position of the signaling domain, and the lack of electron density connecting the signaling to the plug domain in molecule B (Figures 1 and 2). The signaling domain is not at the same location, and two distinct interaction zones between the domain and the rest of the protein are observed (Figure 2). In molecule A, the mixed three-stranded β sheet of the signaling domain forms a four-stranded β sheet with residues of the TonB box (Figure 1D). The fourth strand involves the residues Met131–Thr133. The Ile132 main chain is hydrogen bonded to the Tyr72 main chain, and the Thr133 carbonyl group is hydrogen bonded to the Gln60 side chain. Ile132

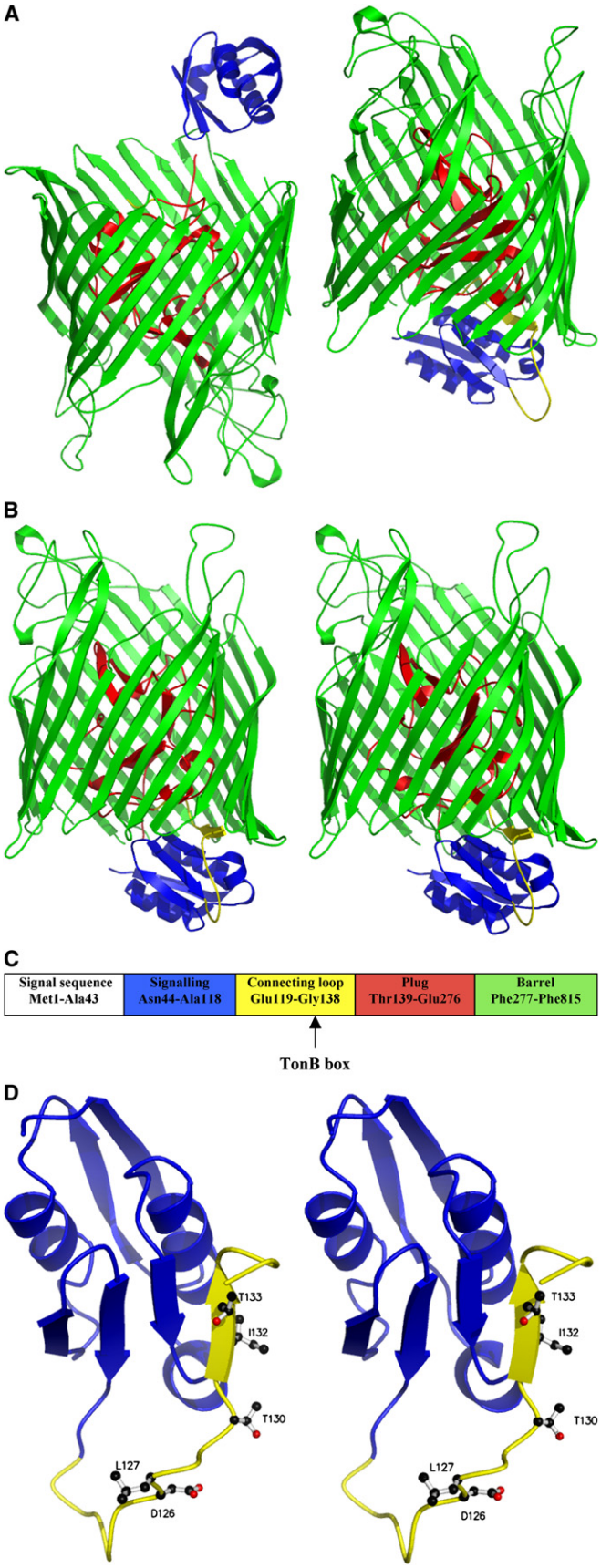

Figure 1. The FpvA Structure in Its Apo Form

(A) A view of the asymmetric unit. The signaling domain is colored blue. The loop connecting the signaling domain to the plug domain is colored yellow (molecule A). The plug is colored red and the barrel is in green.

(B) A stereoview of the full-length FpvA (molecule A).

(C) The FpvA domains (Wirth et al., 2007) including the connecting loop (yellow), which contains the TonB box composed of Asp126, Leu127, Thr130, Ile132, and Thr133 (Ferguson et al., 2007).

(D) A stereoview of the four-stranded β sheet between residues of the TonB box located in a β strand and the three-stranded β sheet of the periplasmic signaling domain. Residues of the TonB box (Ferguson et al., 2007) are drawn in ball-and-stick representations and the connecting loop containing the TonB box is colored yellow.

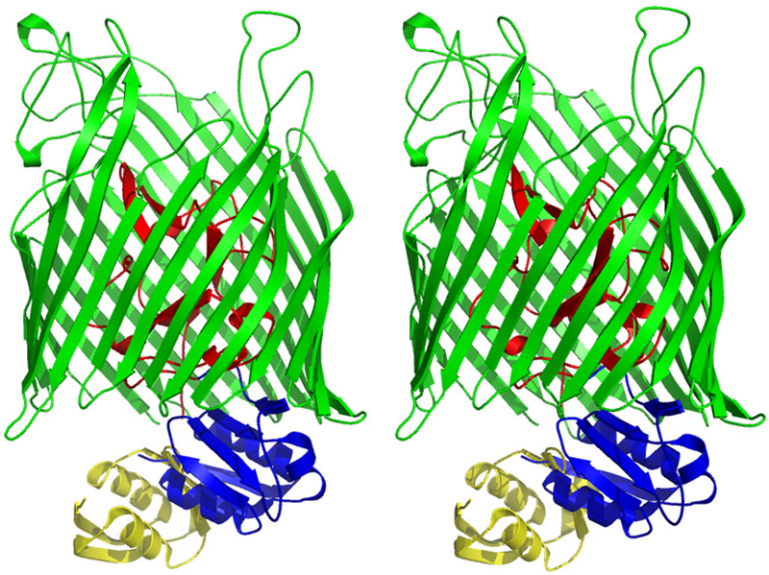

Figure 2. Stereoview of the Superimposition of the FpvA Molecules of the Asymmetric Unit
The two positions of the signaling domain are shown. For clarity, only one barrel and one plug have been drawn.

and Thr133 belong to the TonB box (Ferguson et al., 2007) (Figure 1D).

The signaling domains can be superimposed with a 0.68 Å rsmd value. The largest deviations are observed from Gln109 to Asn111 (as large as 3.43 Å for Gly110). Eighty-one interatomic contacts less than 3.6 Å are observed between Gln44–Gln136 and Leu137–Phe815 in molecule A: 34 can be considered to be hydrogen bonds. In molecule B, 21 interatomic contacts of less than 3.6 Å are observed between Gln44–Val117 and Leu137–Phe815; 6 of these are hydrogen bonds.

Structural Comparisons with FpvA-Pvd and FpvA-Pvd-Fe: Extracellular Conformational Changes Mediate Periplasmic Structural Changes

FpvA and FpvA-Pvd superimpose with an rsmd value of 0.87 Å. Upon Pvd binding, large conformational changes are observed in the Pvd-binding pocket (Figures 3A and 3B). In the plug, Ser224–Ala233 does not superimpose, and large distances of up to 7.50 Å (Tyr231 Cα atom) are observed between equivalent residues (Figures 3A and 3B). In FpvA, the Arg204 guanidinium group is hydrogen bonded to the Ser232 hydroxyl and carbonyl group. In FpvA-Pvd, this interaction does not exist because of the conformational change of the binding pocket and because the Arg204 points toward Pvd. In the barrel, Gly359–Trp362 are not superimposed. In FpvA-Pvd, Trp362 interacts with Pvd: movements of this part of the barrel allow FpvA to bind Pvd. The TonB box no longer interacts with the signaling domain and its conformation is changed.

In the periplasmic domain, Ala129–Gln136 does not superimpose (Figures 3A and 3C). The signaling domain is not observed in FpvA-Pvd, although the core of the plug domain does not show any conformational changes; the conformational changes observed in the extracellular loops can be attributed to crystal packing rather than to Pvd binding.

The rmsd value between FpvA and FpvA-Pvd-Fe is 0.735 Å for all residues. FpvA-Pvd-Fe and FpvA-Pvd superimpose well between residues Thr139 and Phe815, and the differences described between FpvA and FpvA-Pvd are also observed between FpvA and FpvA-Pvd-Fe but particularly in the N-terminal part. Indeed, the FpvA-Pvd-Fe structure was solved for residues Gln44–Ala118 and Thr139–Phe815 (Wirth et al., 2007). The other large difference is the location of the signaling domains, which does not correspond to those observed in FpvA (Figure 4). The rmsd value between the signaling domains is 0.63 Å. The Gly101–Gly103 region does not superimpose.

Structure Comparison with FhuA-TonB and BtuB-TonB: A β Strand Exchange and Conformational Changes Are Required for Signal Transduction

Interactions between FhuA and the periplasmic part of TonB involve the TonB box folded as a β strand with the three-stranded β sheet of the TonB periplasmic part (Pawelek et al., 2006), forming a mixed four-stranded β sheet. A similar topology is observed for the interaction between BtuB and the periplasmic part of TonB (Shultis et al., 2006). However, the location of TonB is different in the two complexes. A part of the TonB box of FpvA is folded as a β strand and interacts with the β sheet of the signaling domain, and in this conformation there is not enough space around the TonB box to bind the TonB periplasmic part. The periplasmic part of FpvA must therefore undergo a conformational change to create the space to bind to TonB.

FpvA-TonB Model Based on Structure Comparisons: A Complex for Transmembrane Signal Transduction

We superimposed FpvA and FpvA-Pvd-Fe onto FhuA-TonB and BtuB-TonB. Only in FpvA-Pvd-Fe is the signaling domain in a position to allow interactions with TonB

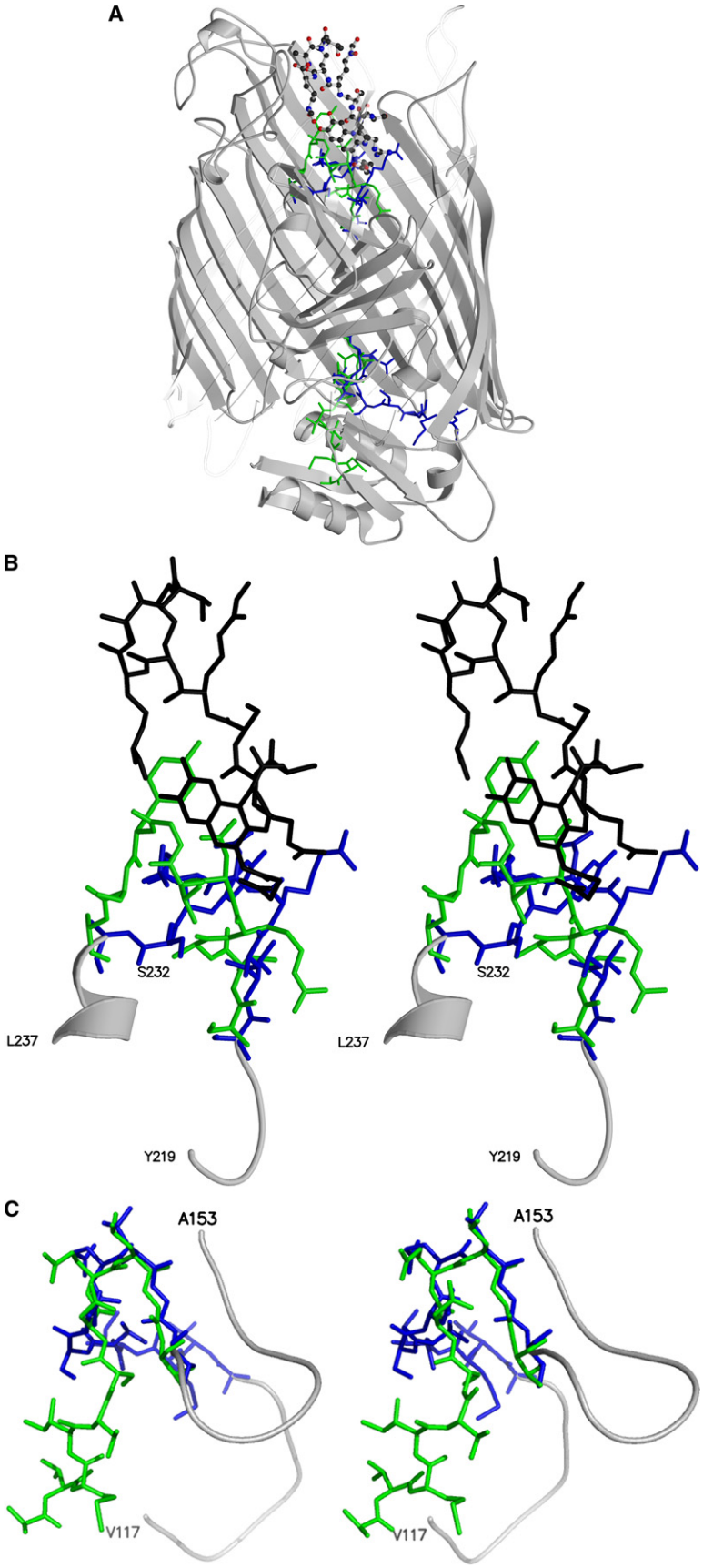

Figure 3. Main Conformational Changes Observed in FpvA upon Pvd Binding

(A) A view of the two main conformational changes.

(B) A stereoview of the conformational change of the main chain from Thr225 to Ala233 in the plug domain. FpvA is colored blue and FpvA-Pvd is in green. The pyoverdine is represented in stick form and is colored black. Tyr219, Ser232, and Leu237 are labeled.

(C) A stereoview of the conformational change observed in the N-terminal part of the plug domain containing residues of the TonB box upon Pvd binding in the extracellular pocket. FpvA is colored blue and FpvA-Pvd is in green. The N-terminal and C-terminal parts are labeled.

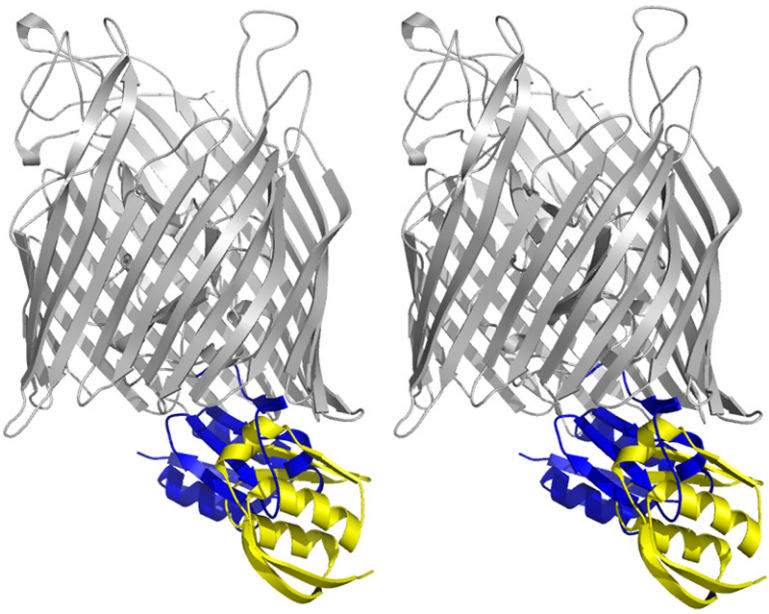

Figure 4. Stereoview of the Superimposition of FpvA onto FpvA-Pvd-Fe
The different positions occupied by the signaling domain are shown. For clarity, only the barrel and plug of FpvA are drawn, and are colored gray. The signaling domain of FpvA-Pvd-Fe is colored yellow.

(Figure 5C). A small number of forbidden contacts are observed between side chains of the periplasmic domain and TonB of FhuA-TonB, and all can be avoided by side-chain rotation. Molecule B of FpvA can be superimposed onto BtuB-TonB, but several forbidden contacts are made between the barrel domain and TonB. Forbidden contacts resulting from the overlap of domains are observed between the periplasmic domain of molecule A and TonB of FhuA-TonB or BtuB-TonB.

DISCUSSION

We crystallized FpvA with two molecules in different conformations in the asymmetric unit. The signaling domain occupies two distinct positions delineating two zones of interactions with the barrel domain. The difference between the two positions probably results from the crystallization conditions (1.3–1.4 M Na_2HPO_4), which may destabilize interactions between the signaling domain and the rest of the protein. This suggests that the interactions between the periplasmic domain and the rest of the protein are weak.

The structure of the TonB box has been completely solved: a part of the TonB box is folded as a β strand in molecule A and interacts with the three-stranded β sheet of the signaling domain (Figure 1D). The absence of electron density for the TonB box in molecule B indicates that it has substantial flexibility, and this may be a consequence of the position of the signaling domain. TonB box flexibility has been suggested previously (Cobessi et al., 2005a) for FpvA-Pvd: in this complex, the TonB box is in an extended conformation and the signaling domain is not observed in the electron density maps. This conformation may allow interactions between TonB and FpvA, and such interactions are necessary for Pvd release (Clement et al., 2004).

Pvd binding leads to conformational changes in its recognition pocket. The main chain from Thr225 to Ala233 in the plug domain and the side chains of several residues undergo conformational changes to create enough space for Pvd binding. In FpvA-Pvd and FpvA-Pvd-Fe, the Arg204 guanidinium group interacts with Pvd. Pvd and Pvd-Fe binding at the extracellular face leads to flexibility of the N-terminal part. This flexibility is even greater in FpvA-Pvd-Fe, in which the TonB box cannot be detected in electron density following Pvd-Fe binding (Wirth et al., 2007), and the signaling domain is located in a different position to that it adopts in FpvA. The flexibilities of the TonB box and signaling domain probably allow FpvA to interact with both (1) FpvR to regulate the expression of PvdS and FpvI, responsible for transcription of pyoverdine biosynthetic genes and *fpva* gene (Redly and Poole, 2005), and (2) TonB for energy transduction. There is no biochemical data available to indicate whether there is formation of a ternary complex between the receptor, TonB, and FpvR or between their counterparts in other bacteria, for example FecA/FecR in *E. coli*. However, the interactions between these three proteins suggest that they are probably in close proximity to each other in the membranes.

The conformation of the N-terminal part of FpvA has to change to allow interactions between TonB and the TonB box; this interaction would otherwise be prevented by interactions between residues of the TonB box and the signaling domain which form a four-stranded β sheet. Structural comparisons with TonB-FhuA and TonB-BtuB suggest that the position of the signaling domain in FpvA also prevents interactions with TonB. Consequently, the signaling domain has to move away from either of the two observed positions in FpvA, to allow the interaction between the TonB box and TonB to take place (Figure 5). The interaction involving the signaling domain is probably

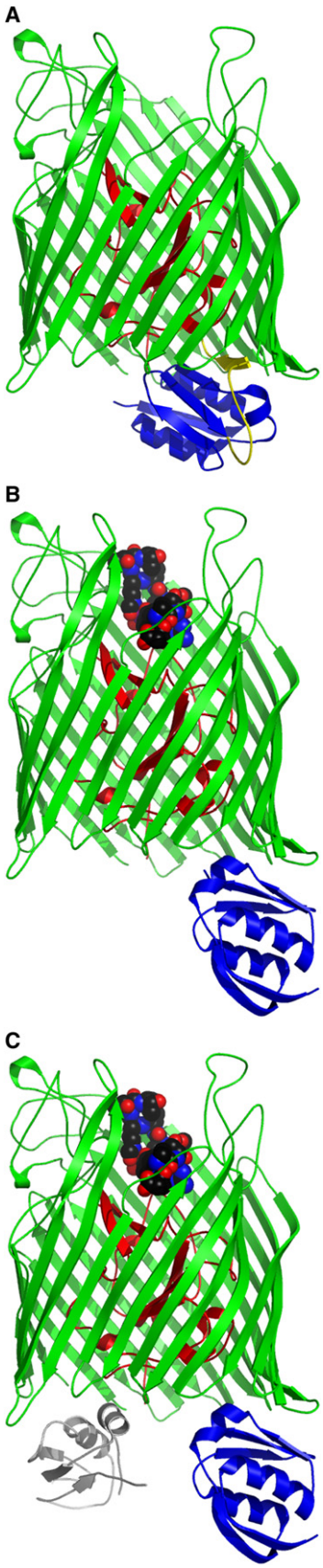

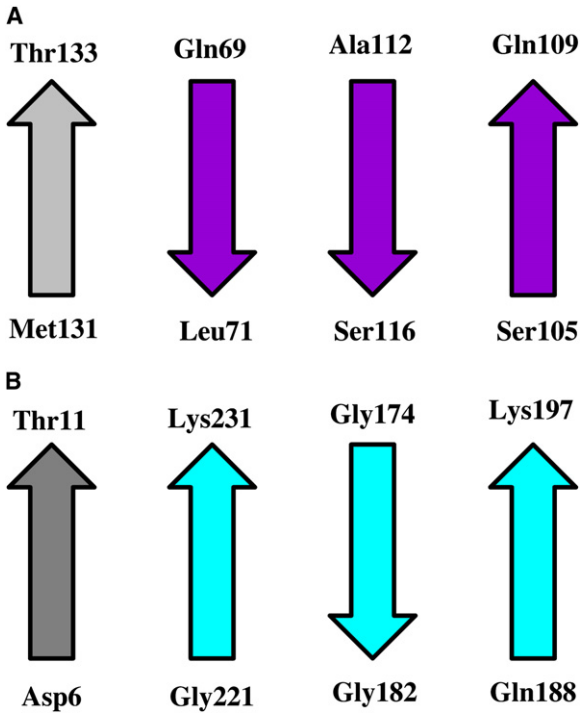

Figure 6. The β Strand Lock Exchange
Topologies of the four-stranded β sheet observed in FpvA between the TonB box and the three-stranded β sheet of the signaling domain (A), and between the TonB box and the TonB periplasmic domain in BtuB-TonB (B). The TonB box is colored gray.

weak, such that it can be displaced to interact with the inner membrane protein FpvR. One of the three observed positions for the periplasmic domain is compatible, according to modeling analyses, with interactions between TonB and the TonB box. The FpvA-Pvd-Fe structure may represent the interactions with the inner membrane proteins TonB and FpvR. It is possible that in such complexes FpvA could also interact with FpvR. Indeed, the two-stranded β sheet of the signaling domain is exposed to the solvent and contains residues which when mutated in FecA (Breidenstein et al., 2006) strongly affect signaling.

The conformational change (Figure 5) is also essential for interactions between TonB and the TonB box. In FpvA, this interaction is prevented by the interaction between residues of the TonB box folded as a β strand and the three-stranded β sheet of the signaling domain. The same type of structural motif (Figure 6) is also observed in the crystal structures of BtuB-TonB and FhuA-TonB:

Figure 5. View of the Sequential Conformational Change that Can Occur upon Pvd-Fe Binding
(A) FpvA: the TonB box is buried.
(B) Fpva-Pvd-Fe: the TonB box is flexible and the signaling domain has moved.
(C) A model of the complex between the periplasmic part of TonB and FpvA-Pvd-Fe based on the superimposition of FpvA-Pvd-Fe onto FhuA-TonB. The periplasmic domain of TonB is colored gray, and a space-filling representation is used for pyoverdine.

there is interaction between the TonB box folded as a β strand and the three-stranded β sheet of the periplasmic part of TonB; however, the structure of the protein complex involving FhuA does not superimpose onto that involving BtuB. To allow interactions through a conserved structural motif and the β strand exchange, the signaling domain must interact with the protein weakly. Sequence analyses do not reveal similarities between the β strands of TonB and the signaling domain involved in interactions with the TonB box. Presumably, therefore, only the conformation of the backbone is important. The core of FpvA shows the same overall conformation in all the structures described. This raises the question of the mechanism involved in the conformational change in the periplasm following the binding of the ligands at the extracellular face of the receptor.

The TonB box may therefore be a lock for signal transduction. Its destabilization after Pvd-Fe binding may allow movements of the signaling domain facilitating interaction with FpvR and, by destabilizing its interactions with the signaling domain, interaction with TonB through a four-stranded β sheet (Figure 5). The interaction between the signaling domain and FpvR leads to the activation of the sigma factors involved in transcription of the *fpva* and pyoverdine biosynthetic genes. The interaction between TonB and the TonB box allows the energy transduction for iron-siderophore transport which necessitates a conformational change of the receptor. These observations and considerations suggest that there is a sequential mechanism for the conformational changes coupled to the transport and signal transduction involving FpvR and TonB.

EXPERIMENTAL PROCEDURES

Expression and Purification

The plasmid pPVR2, carrying the *fpvA* gene under the control of its own promoter (Poole et al., 1993), was used to transform the *P. aeruginosa pvdA*-deficient mutant PAD06 by an $MgCl_2$-based method (Mercer and Loutit, 1979). These strains are unable to synthesize Pvd and overproduce FpvA when grown in a succinate medium (Demange et al., 1990). FpvA was purified as described previously for FptA (Cobessi et al., 2005b), with an additional anion-exchange chromatography step after gel filtration. At the end of the purification, ultrafiltration at 10,000 × g was used for detergent exchange with a 50 kDa molecular weight cutoff (Amicon, Millipore).

Crystallization

Initial screening was conducted at 293K using the sitting-drop vapor-diffusion method and the sparse-matrix sampling approach (Jancarik and Kim, 1991) with the Classic, Classic Lite, MbClass, and MbClass II sparse matrices from Nextal; 0.5% and 1% C8E4 or C8E5 were used. Aliquots of 0.5 μl of protein solution were mixed with an equal reservoir volume in 96-well plates, and several crystallization conditions were found. Crystallization conditions were refined using Cryshem plates and the sitting-drop vapor-diffusion method by mixing 0.5, 1, or 2 μl of protein solution with an equal reservoir volume, and the samples were equilibrated with the same precipitant. Crystals of FpvA were obtained by mixing 1.3–1.4 M NaH_2PO_4, 0.1 M MES (pH 6.5) with 5 mg/ml FpvA in 1% C8E5.

Data Collection

Prior to data collection, crystals of FpvA were soaked in a solution containing 30% glycerol as the cryoprotection agent. X-ray diffraction experiments were performed at 100K with crystals mounted in cryoloops and flash-frozen in liquid nitrogen. The data were collected on beamline ID23-1 at the European Synchrotron Radiation Facility. The data were processed using XDS (Kabsch, 1993) and scaled using SCALA (Evans, 1993). Statistics concerning data reduction and merging are summarized in Table 1.

Structure Resolution and Refinement

The structure was solved by molecular replacement using MOLREP (Vagin and Teplyakov, 1997) from CCP4 (1994) and the residues from Thr139 to Phe815 of FpvA-Pvd-Fe as a molecular model (Wirth et al., 2007). The signaling domain and the connecting loop between the signaling domain and the plug were added in the $2F_o - F_c$ electron density map. The model was rebuilt using O (Jones et al., 1991) and cycles of translation/libration/screw refinement and energy minimization were carried out using REFMAC5 (Murshudov et al., 1997). The atomic coordinate file contains two FpvA molecules with the residues Gln44–Phe815 (molecule A), Gln44–Val117 and Gln136–Phe815 (molecule B), as well ten phosphate ions and one detergent molecule.

Model quality was assessed using PROCHECK (Laskowski et al., 1993) and WHATCHECK (Hooft et al., 1996). The majority of residues (87.7%) are in the most favored parts of the Ramachandran plot, 12.2% are in allowed regions, and no residue is found in disallowed regions. At the end of the refinement, the R and R_{free} (Brunger, 1992) factors were 20.8% and 24.7%, respectively (Table 2). The interactions between residues were found using CONTACT from CCP4 and a 3.6 Å distance cutoff. All the drawings were prepared using MOLSCRIPT (Kraulis, 1991), PyMOL (DeLano, 2002), Raster3D (Merritt and Murphy, 1994), and CCP4. The atomic coordinates and structure factors have been deposited in the Protein Data Bank (Berman et al., 2000) under ID code 2O5P.

ACKNOWLEDGMENTS

We thank the staff of the ID23-1 beamline at the ESRF for their kind assistance during data collection, and the "European Community—Research Infrastructure Action" under FP6 "Structuring the European Research Area Programme" contract RII3/CT/2004/5060008. This work was supported by the Association Française de Lutte contre la Mucovicidose (AFLM), the ACI Interface Physique, Chimie, Biologie and the Dynamique et Réactivité des Assemblages Biologiques program of the Ministère de l'Enseignement Supérieur, de la Recherche et de la Technologie, and the Centre National de la Recherche Scientifique.

Received: July 19, 2007
Revised: August 27, 2007
Accepted: August 27, 2007
Published: November 13, 2007

REFERENCES

Berman, H.M., Westbrook, J., Feng, Z., Gilliland, G., Bhat, T.N., Weissig, H., Shindyalov, I.N., and Bourne, P. (2000). The Protein Data Bank. Nucleic Acids Res. *28*, 235–242.

Braun, V., Mahren, S., and Ogierman, M. (2003). Regulation of the FecI-type ECF sigma factor by transmembrane signaling. Curr. Opin. Microbiol. *6*, 173–180.

Breidenstein, E., Mahren, S., and Braun, V. (2006). Residues involved in FecR binding are localized on one side of the FecA signaling domain in *Escherichia coli*. J. Bacteriol. *188*, 6440–6442.

Brunger, A.T. (1992). The R_{free} value: a novel statistical quantity for assessing the accuracy of crystal structures. Nature *355*, 472–475.

CCP4 (Collaborative Computational Project, Number 4) (1994). The CCP4 suite: programs for protein crystallography. Acta Crystallogr. D Biol. Crystallogr. *50*, 760–763.

Clement, E., Mesini, P.J., Pattus, F., and Schalk, I.J. (2004). The binding mechanism of pyoverdin with the outer membrane receptor FpvA in *Pseudomonas aeruginosa* is dependent on its iron-loaded status. Biochemistry *43*, 7954–7965.

Cobessi, D., Celia, H., Folschweiler, N., Schalk, I.J., Abdallah, M.A., and Pattus, F. (2005a). The crystal structure of the pyoverdine outer membrane receptor FpvA from *Pseudomonas aeruginosa* at 3.6 Å resolution. J. Mol. Biol. *347*, 121–134.

Cobessi, D., Celia, H., and Pattus, F. (2005b). Crystal structure at high resolution of ferric-pyochelin and its membrane receptor FptA from *Pseudomonas aeruginosa*. J. Mol. Biol. *352*, 893–904.

DeLano, W.L. (2002). The PyMOL Molecular Graphics System (Palo Alto, CA: DeLano Scientific).

Demange, P., Bateman, A., Mertz, C., Dell, A., Piemont, Y., and Abdallah, M.A. (1990). Bacterial siderophores: structures of pyoverdins Pt, siderophores of *Pseudomonas tolaasii* NCPPB 2192, and pyoverdins Pf, siderophores of *Pseudomonas fluorescens* CCM 2798. Identification of an unusual natural amino acid. Biochemistry *29*, 11041–11051.

Evans, P.R. (1993). Data reduction. In Proceedings of CCP4 Study Weekend on Data Collection and Processing, L. Sawyer, N. Isaacs, and S. Bailey, eds. (Warrington, UK: Daresbury Laboratory), pp. 114–122.

Ferguson, A.D., and Deisenhofer, J. (2002). TonB-dependent receptors—structural perspectives. Biochim. Biophys. Acta *1565*, 318–332.

Ferguson, A.D., and Deisenhofer, J. (2004). Metal import through microbial membranes. Cell *116*, 15–24.

Ferguson, A.D., Chakraborty, R., Smith, B.S., Esser, L., Van der Helm, D., and Deisenhofer, J. (2002). Structural basis of gating by the outer membrane transporter FecA. Science *295*, 1715–1719.

Ferguson, A.D., Amezcua, C.A., Halabi, N.M., Chelliah, Y., Rosen, M.K., Ranganathan, R., and Deisenhofer, J. (2007). Signal transduction pathway of TonB-dependent transporters. Proc. Natl. Acad. Sci. USA *104*, 513–518.

Garcia-Herrero, A., and Vogel, H.J. (2005). Nuclear magnetic resonance solution structure of the periplasmic signalling domain of the TonB-dependent outer membrane transporter FecA from *Escherichia coli*. Mol. Microbiol. *58*, 1226–1237.

Hooft, R.W.W., Vriend, G., Sander, C., and Abola, E.E. (1996). Errors in protein structures. Nature *381*, 272.

Jancarik, J., and Kim, S.H. (1991). Sparse matrix sampling: a screening method for crystallization of proteins. J. Appl. Crystallogr. *24*, 409–411.

Jones, T.A., Zou, J.Y., Cowan, S.W., and Kjeldgaard, M. (1991). Improved methods for building protein models in electron density maps and the location of errors in these models. Acta Crystallogr. A *47*, 110–119.

Kabsch, W. (1993). Automatic processing of rotation diffraction data from crystals of initially unknown symmetry and cell constants. J. Appl. Crystallogr. *26*, 795–800.

Koebnik, R. (2005). TonB-dependent trans-envelope signalling: the exception or the rule? Trends Microbiol. *13*, 343–347.

Kraulis, P.J. (1991). MOLSCRIPT: a program to produce both detailed and schematic plots of protein structures. J. Appl. Crystallogr. *24*, 946–950.

Laskowski, R.A., MacArthur, M.W., Moss, D.S., and Thornton, J.M. (1993). PROCHECK: a program to check the stereochemical quality of protein structures. J. Appl. Crystallogr. *26*, 283–291.

Mercer, A.A., and Loutit, J.S. (1979). Transformation and transfection of *Pseudomonas aeruginosa*: effects of metal ions. J. Bacteriol. *140*, 37–42.

Merritt, E.A., and Murphy, M.E.P. (1994). Raster3D version 2.4—a program for photorealistic molecular graphics. Acta Crystallogr. D Biol. Crystallogr. *50*, 869–873.

Murshudov, G.N., Vagin, A.A., and Dodson, E.J. (1997). Refinement of macromolecular structures by the maximum-likelihood method. Acta Crystallogr. D Biol. Crystallogr. *53*, 240–255.

Neilands, J.B. (1995). Siderophores, structure and function of microbial iron transport compounds. J. Biol. Chem. *270*, 26723–26726.

Pawelek, P.D., Croteau, N., Ng-Thow-Hing, C., Khursigara, C.M., Moiseeva, N., Allaire, M., and Coulton, J.W. (2006). Structure of TonB in complex with FhuA, *E. coli* outer membrane receptor. Science *312*, 1399–1402.

Poole, K., and McKay, G.A. (2003). Iron acquisition and its control in *Pseudomonas aeruginosa*: many roads lead to Rome. Front. Biosci. *8*, D661–D686.

Poole, K., Neshat, S., Krebes, K., and Heinrichs, D.E. (1993). Cloning and nucleotide sequence analysis of the ferripyoverdine receptor gene FpvA of *Pseudomonas aeruginosa*. J. Bacteriol. *175*, 4597–4604.

Posey, J.E., and Gherardini, F.C. (2000). Lack of a role for iron in the Lyme disease pathogen. Science *288*, 1651–1653.

Redly, G.A., and Poole, K. (2005). FpvIR control of fpvA ferric pyoverdine receptor gene expression in *Pseudomonas aeruginosa*: demonstration of an interaction between FpvI and FpvR and identification of mutations in each compromising this interaction. J. Bacteriol. *187*, 5648–5657.

Schalk, I.J., Kyslik, P., Prome, D., Van Dorssealer, A., Poole, K., Abdallah, M.A., and Pattus, F. (1999). Copurification of the FpvA ferric pyoverdin receptor of *Pseudomonas aeruginosa* with its iron-free ligand: implication for siderophore-mediated iron transport. Biochemistry *38*, 9357–9365.

Schalk, I.J., Yue, W.W., and Buchanan, S.K. (2004). Recognition of iron-free siderophores by TonB-dependent iron siderophores. Mol. Microbiol. *54*, 14–22.

Shultis, D.D., Purdy, M.D., Banchs, C.N., and Wiener, M.C. (2006). Outer membrane active transport: structure of the BtuB:TonB complex. Science *312*, 1396–1399.

Stintzi, A., Barnes, C., Xu, J., and Raymond, K.N. (2000). Microbial iron transport via a siderophore shuttle: a membrane ion transport paradigm. Proc. Natl. Acad. Sci. USA *97*, 10691–10696.

Vagin, A., and Teplyakov, A. (1997). MOLREP: an automated program for molecular replacement. J. Appl. Crystallogr. *30*, 1022–1025.

Wirth, C., Meyer-Klaucke, W., Pattus, F., and Cobessi, D. (2007). From the periplasmic signaling domain to the extracellular face of an outer membrane signal transducer of *Pseudomonas aeruginosa*: crystal structure of the ferric pyoverdine outer membrane receptor. J. Mol. Biol. *368*, 398–406.

Yue, W.W., Grizot, S., and Buchanan, S.K. (2003). Structural evidence for iron-free citrate and ferric citrate binding to the TonB-dependent outer membrane transporter FecA. J. Mol. Biol. *332*, 353–368.

Accession Numbers

The atomic coordinates and structure factors of FpvA in its apo form have been deposited in the Protein Data Bank under ID code 2O5P.